Original Article

Curcuma xanthorrhiza extract and xanthorrhizol ameliorate cancer-induced adipose wasting in CT26-bearing mice by regulating lipid metabolism and adipose tissue browning

Haeun Kim [a], Dong-Woo Lee [a,b], Jae-Kwan Hwang [a,*]

[a] *Graduate School of Bioindustrial Engineering, Yonsei University, Seoul, Republic of Korea*
[b] *Department of Biotechnology, Yonsei University, Seoul, Republic of Korea*

ABSTRACT

Background: Cancer cachexia—characterized by anorexia, body weight loss, skeletal muscle atrophy, and fat loss—affects nearly 80% of cancer patients and accounts for 20% of cancer deaths. *Curcuma xanthorrhiza*, known as Java turmeric, and its active compound xanthorrhizol (XAN) exhibit anticancer, anti-inflammatory, and antioxidant properties. However, the ameliorative effects of *C. xanthorrhiza* extract (CXE) and XAN on cancer-associated adipose atrophy remain unexplored. This study aimed to evaluate the therapeutic effects of CXE and XAN on cancer cachexia-induced adipose tissue wasting in CT26 tumor-bearing mice.
Methods: CT26 cells were injected subcutaneously into the right flank of BALB/c mice to establish a cancer cachexia model. To evaluate the inhibitory effects of CXE and XAN on cancer cachexia, 50 and 100 mg/kg CXE and 15 mg/kg XAN were administered orally every day for 1 week.
Results: CXE and XAN administration significantly attenuated the loss of body weight and epididimal fat mass by cancer cachexia. In epididymal adipose tissues, administration of CXE or XAN inhibited white adipose tissue browning by repressing expression of the thermogenic genes. Simultaneously, CXE or XAN attenuated fat catabolism through the downregulation of lipolytic genes. The administration of CXE or XAN induced the expression of genes associated with adipogenesis and lipogenesis-related genes. Moreover, CXE or XAN treatment was associated with maintaining metabolic homeostasis; regulating the expression of adipokines and AMP-activated protein kinase (AMPK).
Conclusions: CXE and XAN mitigate cancer-induced adipose tissue atrophy, primarily by modulating lipid metabolism and WAT browning, indicating their therapeutic potential for cachectic cancer patients.

1. Introduction

Cancer cachexia, a multifactorial catabolic disease, is associated with progressive weight loss, involving the depletion of adipose tissue and skeletal muscle. Cancer cachexia is present in 50% to 80% of advanced cancer patients and contributes to 20% of mortalities among cancer patients.[1] While previous research has primarily focused on cancer-induced skeletal muscle atrophy, recent studies are emphasizing the significance of adipose tissue depletion in the progression of cancer cachexia. Clinical studies have demonstrated a strong correlation between the loss of adipose tissue and increased mortality in cachectic cancer patients.[2] Additionally, several studies have suggested that cancer patients with normal or low body mass index are at a greater risk of mortality compared to obese patients.[3] The molecular mechanisms underlying cancer-associated adipose atrophy have been elucidated, but dysregulated lipid metabolism and browning of white adipose tissue (WAT) have been identified as key factors contributing to the progression of cancer cachexia.[4]

Despite numerous studies and clinical trials, there are currently no approved medications or established standard treatments for cancer cachexia. Recently, there has been significant interest in exploring the potential of herbal medicines, natural products, and bioactive compounds to act as treatments for cancer cachexia. As systemic inflammation and oxidative stress are considered crucial therapeutic targets for cancer cachexia, natural products with anti-inflammation and antioxidant properties could potentially alleviate cachectic symptoms.[1]

Curcuma xanthorrhiza Roxb., a member of the Zingiberaceae family, is also known as Java turmeric or Temulawak and is mainly distributed in Indonesia, Malaysia, and Thailand.[5] Xanthorrhizol (XAN), a natural sesquiterpenoid, is the major bioactive compound present in

C. xanthorrhiza.[6] Both *C. xanthorrhiza* and xanthorrhizol have been reported to exhibit anti-inflammatory and anti-oxidative effects in various in vivo and in vitro models.[6–9] Additionally, they have demonstrated anticancer properties by inhibiting cancer cell proliferation and promoting apoptosis in different cancer cell lines.[10, 11] Notably, xanthorrhizol has shown a protective effect against cisplatin, a commonly used chemotherapy agent, suggesting its potential to ameliorate both chemotherapy- and cancer-induced cachexia.[12] However, the effect of *C. xanthorrhiza* extract (CXE) and XAN on cancer cachexia remains unexplored. This study aimed to assess the therapeutic effect of CXE and XAN on cancer cachexia-associated adipose atrophy and the underlying mechanisms in CT26-bearing mice.

2. Methods

2.1. Chemical reagents and antibodies

Antibodies against HSL (# 4107S), phospho-HSL (# 4126S), ATGL (# 2138S), AMPK (# 2532S), and phospho-AMPK (# 2531S) were purchased from Cell Signaling Technology (Beverly, MA, USA). Anti-α-tubulin (# D0921) primary antibodies were obtained from Santa Cruz Biotechnology Inc. (Santa Cruz, CA, USA). Horseradish peroxidase-linked secondary antibodies were obtained from Bethyl Laboratories, Inc. (Montgomery, TX, USA). Enhanced chemiluminescence (ECL) solution and NP-40 buffer were obtained from ELPIS Biotech (Daejeon, Korea).

2.2. Preparation of CXE and XAN

Dried rhizomes of *Curcuma xanthorrhiza* weighing 200 g were obtained from Phytomedi Inc. (Seoul, Korea) and subjected to extraction using a supercritical carbon dioxide extraction process. The extraction was carried out at a temperature of 50 °C and a pressure of 40 MPa for a duration of 4 h. The resulting extract, referred to as CXE, had a yield of 8.0% (w/w). The content of xanthorrhizol (XAN) in CXE was determined to be 30.0% (w/w). The isolation of XAN from the rhizomes of *C. xanthorrhiza* followed a previously established method outlined in Kim et al.[6]

2.3. Animal studies

Eight-week-old male BALB/c mice were obtained from Orient Bio (Sungnam, Korea) and housed in the Yonsei Laboratory Animal Research Center (YLARC; Seoul, Korea) under controlled conditions of temperature (23 ± 2 °C) and humidity (55% ± 5%) and a 12-h light-dark cycle. The mice were acclimated for 1 week prior to the injection of CT26 cells. Following a week of acclimatization, mice were divided into five distinct treatment groups. (i) CON: the healthy control and was treated with saline; (ii) CC (cancer cachexia): injected with CT26 cells to induce cancer cachexia and treated with saline; (iii) CXE50: injected with CT26 cells and received daily treatment of 50 mg/kg of CXE; (iv) CXE100: was injected with CT26 cells and received daily treatment of 100 mg/kg of CXE daily; (v) XAN15: injected with CT26 cells and received daily treatment of 15 mg/kg/day of XAN. On day 0, 5×10^6 CT26 cells were subcutaneously injected into the right flank of the mice. Tumor growth became palpable 9 days after cell inoculation. Throughout the experiment, the body weight of the mice was measured every other day. Treatment with CXE and XAN began 14 days after tumor inoculation. CT26-bearing mice were orally administered either 50 or 100 mg/kg of CXE or 15 mg/kg of XAN for a period of 7 days. At the end of the experiment, the mice were sacrificed under anesthesia by cardiac puncture. The tumor and epididymal fat were collected and stored at −80 °C for subsequent molecular and histological analysis. The experimental protocol was approved by the Institute of Animal Care and Use Committee (IACUC) of Yonsei University (Seoul, Korea) (IACUC-202212-1592-02) to ensure ethical treatment of the animals.

Table 1
Sequences of forward and reverse primers for RT-PCR analysis.

Origin	Gene	Direction	Sequence (5′–3′)
Mouse	UCP-1	Forward	AAGAGCTGATGAAGTCCAGACAG
		Reverse	TTATTCGTGGTCTCCCAGCATAG
	PGC-1α	Forward	GCTGAAGAGGCAAGAGACAGAA
		Reverse	TGGAAATGCTGCCATTTGAAGG
	PPARγ	Forward	CGAATTTTTCAAGGGTGCCAGT
		Reverse	CTTTTGAGGAACTCCCTGGTCA
	C/EBPα	Forward	CTAGGAGATTCCGGTGTGGC
		Reverse	CCCGAGAGGAAGCAGGAATC
	SREBP-1c	Forward	GCTGTTGGCATCCTGCTATCT
		Reverse	AGCCAATGACAAAGGTCCTCAA
	LPL	Forward	AAGCCCCACAAGTGTAGTCG
		Reverse	ATAATGGGGATGCCGGTGAC
	FAS	Forward	CAAGACGAAAATGATGCTTGGGT
		Reverse	ATAAGTATCAGAGCCTGAAGCCG
	ACC	Forward	CTATAGGATCACACAGC CCAGTC
		Reverse	GTAAGACCTCATGGTACAGGCAA
	Adiponectin	Forward	ATGAAAGATGTGAAGGTGAGCCT
		Reverse	TGTGTCGACTGTTCCATGATTCT
	Leptin	Forward	CATTCTGTGGGGAGTTTTGTTCC
		Reverse	TTCCATCAAGTGTCCTCTCACTG
	β-actin	Forward	AAGTACTCTGTGTGGATCGGTG
		Reverse	AAACGCAGCTCAGTAACAGTCC

2.4. Western blot analysis

Epididymal adipose tissues were homogenized in NP40 lysis buffer containing a proteinase inhibitor cocktail. The resulting protein lysates were clarified by centrifugation at 13,000 rpm for 10 min at 4 °C, and the supernatants were used for western blot analysis. The protein concentration was determined using the Bradford assay (Bio-Rad Laboratories Inc., Hercules, CA, USA), and the proteins were then separated by sodium dodecyl sulfate-polyacrylamide gel electrophoresis (SDS-PAGE). The separated proteins in the gel were transferred onto 0.45-μm nitrocellulose membranes (GE Healthcare, Piscataway, NJ, USA), which were subsequently blocked with 5% skimmed milk for at least 1 h at room temperature. The membranes were incubated overnight at 4 °C with primary antibodies against HSL, p-HSL, ATGL, AMPK, p-AMPK, and α-tubulin (dilution 1:1000) under gentle agitation. Subsequently, the membranes were incubated with secondary antibodies (dilution 1:5000) at 4 °C for 2 h. The target proteins were detected using an enhanced chemiluminescence (ECL) solution and visualized using the G:BOX imaging analysis system (Syngene, Cambridge, UK). The band densities were quantified using ImageJ software (National Institutes of Health, Bethesda, MD, USA).

2.5. Reverse transcription-polymerase chain reaction (RT-PCR)

Total RNA was extracted from epididymal adipose tissues using TRIzol reagent (Takara Bio, Otsu, Japan) following the manufacturer's instructions. The concentration of isolated RNA was determined using the NanoDrop Lite spectrophotometer (Thermo Fisher Scientific Inc., Waltham, MA, USA). Reverse transcription of RNA into complementary DNA (cDNA) was performed using the RT-Premix (ELPIS Biotech) at 42 °C for 60 min, followed by a 5-min incubation at 95 °C. Quantitative polymerase chain reaction (PCR) amplification was carried out using the synthesized cDNA with the SafeDry Taq PCR premix (CellSafe, Gyeonggi, Korea) and primers (Bioneer, Daejeon, Korea) according to the following protocol: initial enzyme activation at 95 °C for 5 min, denaturation at 95 °C for 30 s, annealing at 53–56 °C for 30 s, extension at 72 °C for 45 s, and final extension at 72 °C for 5 min. The primer sequences used for amplification are provided in Table 1. The final PCR products were stained with Loading STAR dye (DyneBio) and separated by electrophoresis using a 2% agarose gel. The PCR bands were visualized using the G:BOX imaging analysis system (Syngene), and
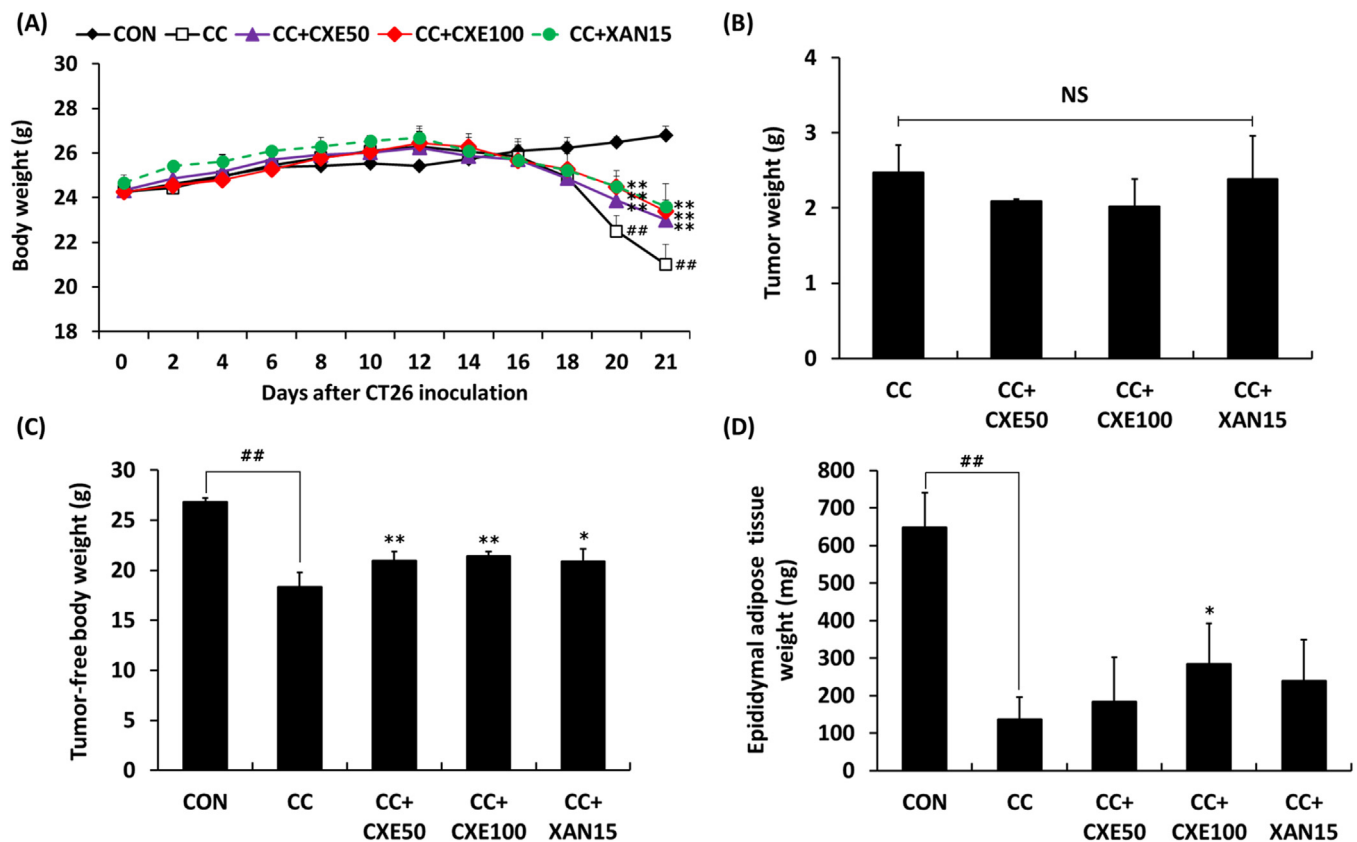
Fig. 1. Effects of CXE and XAN on cachectic phenotypes in CT26-bearing mice. (A) Body weight was measured every other day for 3 weeks. On day 21 after CT26 inoculation, (B) tumor weight, (C) tumor-free body weight, and (D) epididymal adipose tissue weight were measured. Group differences were assessed using a one-way analysis of variance (ANOVA), followed by Duncan's multiple range test. ## $p < 0.01$ (CON group vs. CC group); * $p < 0.05$, ** $p < 0.01$ (CC group vs. CXE- and XAN-treated groups); NS, not significant.

quantification was performed using ImageJ software (National Institutes of Health).

2.6. Statistical analysis

All experimental data are presented as mean values ± standard deviations and were analyzed using SPSS software (IBM Corp., Armonk, NY, USA). Group differences were assessed using a one-way analysis of variance (ANOVA), followed by Duncan's multiple range test. Statistical significance was considered when the p-value was less than 0.05.

3. Results

3.1. CXE and XAN ameliorated the cachectic phenotype in CT26-bearing mice

The CXE and XAN treatments effectively ameliorated the body weight loss in tumor-bearing mice; the body weight of the CC + CXE (both low and high) and CC + XAN15 groups was significantly higher than that of the CC group after 14 days (Fig. 1A). CXE administration slightly decreased tumor weight; however, there was no statistically significant difference between the CC group and CC + CXE50, CC + CXE100, or CC + XAN15 group at the end of the experiment (Fig. 1B). As shown in Fig. 1C, tumor-free body mass in the CC group decreased by 24% compared to pre-inoculation weight, whereas the tumor-free body weight of the CXE- and XAN-treated groups significantly increased compared to the CC group (mean loss rate: CC + CXE50, 13.9%; CC + CXE100, 11.8%; CC + XAN15, 15.3%). The presence of CT26 tumors led to a marked decrease in epididymal fat mass, indicating

adipose tissue wasting (Fig. 1D). Supplementation of 100 mg/kg CXE effectively protected against epididymal adipose tissue loss ($p < 0.05$). Although administration of CXE at 50 mg/kg or XAN at 15 mg/kg slightly attenuated fat loss in CT26-bearing mice, the difference in epididymal fat weight between the CC + CXE50, CC + XAN15, and CC groups was not significant (Fig. 1D).

3.2. CXE and XAN alleviated lipolysis and WAT browning in CT26-bearing mice

As shown in Fig. 2A, western blot analysis of total lysates from epidydimal tissue confirmed a dramatically elevated level of p-HSL and ATGL in CT26-bearing mice. In contrast with the CC group, all groups administered CXE or XAN demonstrated a substantial reduction in the expression of metabolic lipases (Fig. 2A).

The mRNA levels of PGC-1α and UCP1 were significantly elevated in the adipose tissue of CC mice, indicating increased thermogenesis and energy expenditure in tumor-bearing mice (Fig. 2B). However, administration of CXE or XAN resulted in a significant decrease in the expression of PGC-1α and UCP1, suggesting a potential inhibition of WAT browning.

3.3. CXE and XAN enhanced lipogenesis and adipogenesis in CT26-bearing mice

As shown in Fig. 3A, a significant decrease in the gene expression of lipogenic factors was observed in the WAT of CC mice ($p < 0.01$). However, this downregulation was effectively reversed with the administration of CXE or XAN. Notably, groups administered CXE demonstrated a dose-dependent increase in gene expression (Fig. 3A).
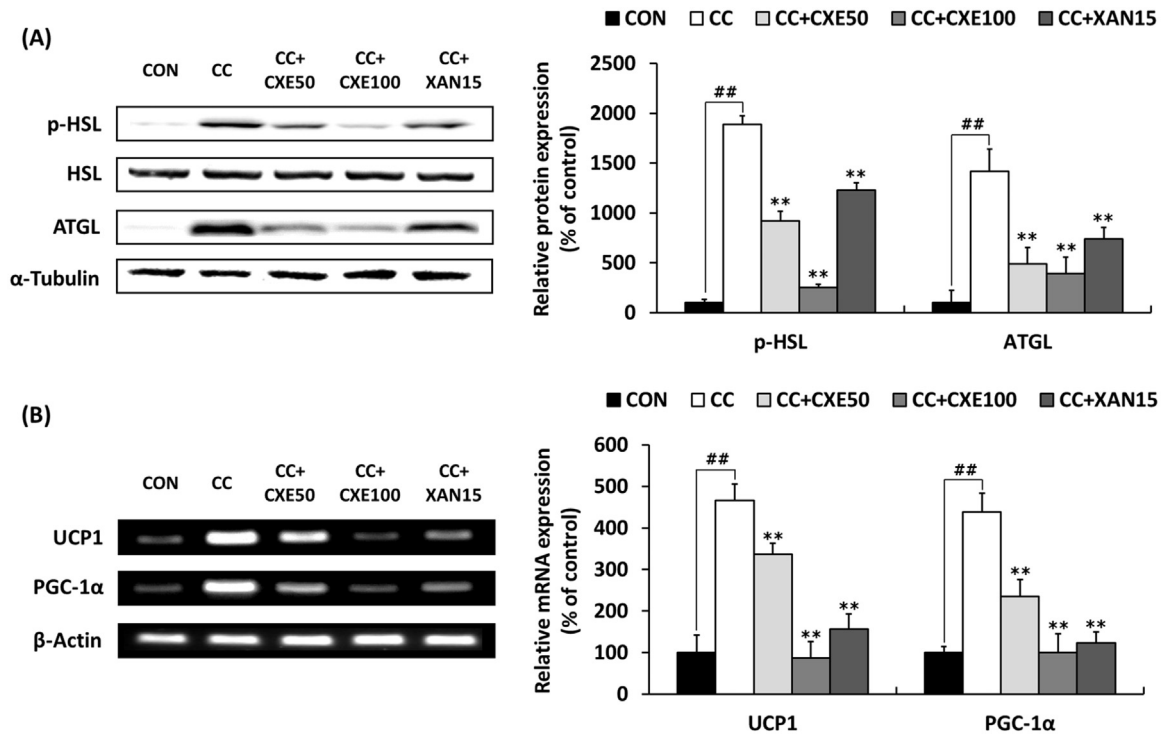
Fig. 2. Effects of CXE and XAN on lipolysis and WAT browning in CT26-bearing mice. (A) p-HSL and ATGL protein expression was analyzed through western blot analysis, with α-tubulin used as the housekeeping gene. (B) UCP-1 and PGC-1α mRNA expression was analyzed through reverse transcription-polymerase chain reaction (RT-PCR), with β-actin used as the housekeeping gene. Group differences were assessed using a one-way analysis of variance (ANOVA), followed by Duncan's multiple range test. ## $p < 0.01$ (CON group vs. CC group); ** $p < 0.01$ (CC group vs. CXE- and XAN-treated groups).
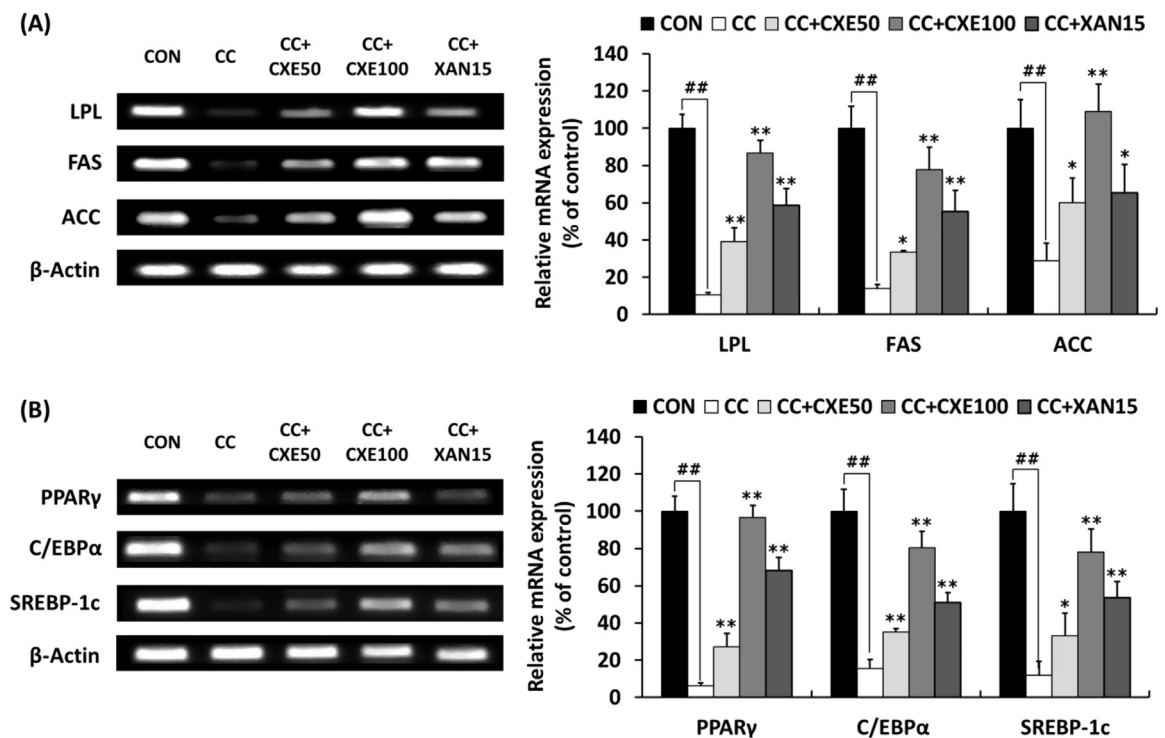

Fig. 3. Effects of CXE and XAN on lipogenesis and adipogenesis in CT26-bearing mice. (A) LPL, FAS, ACC, (B) PPARγ, C/EBPα, and SREBP-1c mRNA expression was analyzed through reverse transcription-polymerase chain reaction (RT-PCR), with β-actin used as the housekeeping gene. Group differences were assessed using a one-way analysis of variance (ANOVA), followed by Duncan's multiple range test. ## $p < 0.01$ (CON group vs. CC group); * $p < 0.05$, ** $p < 0.01$ (CC group vs. CXE- and XAN-treated groups).
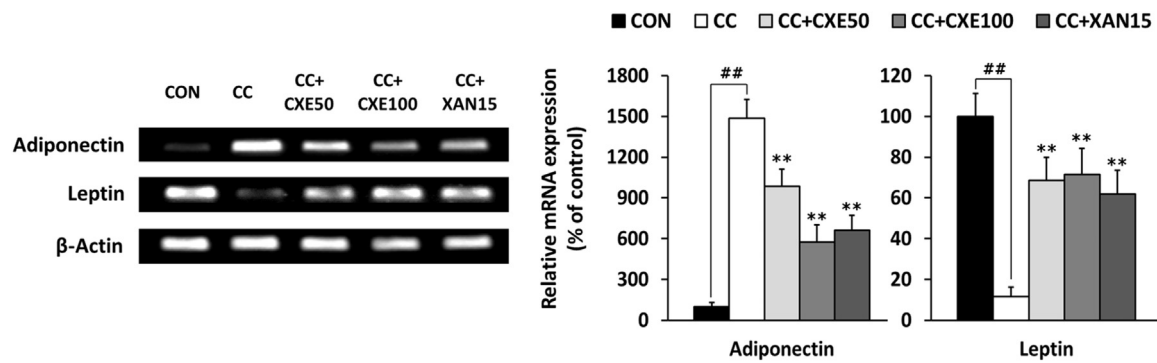
Fig. 4. Effects of CXE and XAN on adipokine production in CT26-bearing mice. Leptin and adiponectin mRNA expression was analyzed through reverse transcription-polymerase chain reaction (RT-PCR), with β-actin used as the housekeeping gene. Group differences were assessed using a one-way analysis of variance (ANOVA), followed by Duncan's multiple range test. ## $p < 0.01$ (CON group vs. CC group); ** $p < 0.01$ (CC group vs. CXE- and XAN-treated groups).
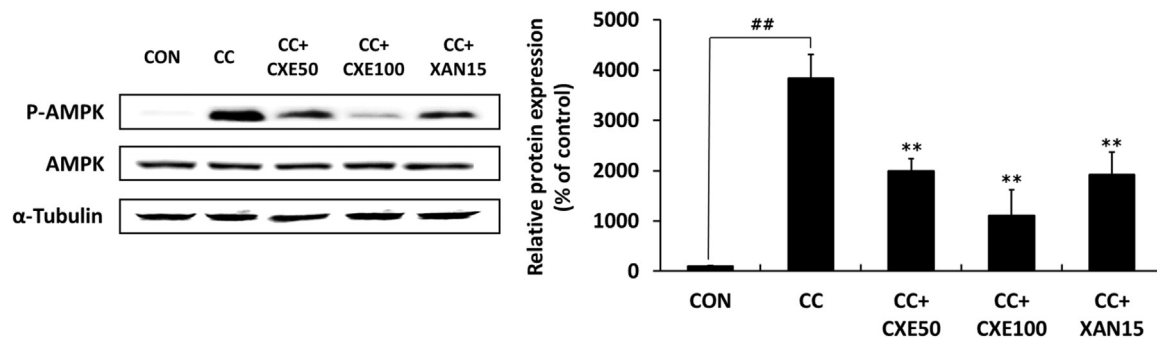

Fig. 5. Effects of CXE and XAN on AMPK expression in CT26-bearing mice. p-AMPK protein expression was analyzed through western blot analysis, with α-tubulin used as the housekeeping gene. Group differences were assessed using a one-way analysis of variance (ANOVA), followed by Duncan's multiple range test. ## $p < 0.01$ (CON group vs. CC group); ** $p < 0.01$ (CC group vs. CXE- and XAN-treated groups).

As depicted in Fig. 3B, the mRNA levels of PPARγ, C/EBPα, and SREBP-1c in the CC group significantly diminished by 93.6% ($p < 0.01$), 84.3% ($p < 0.01$), and 88.1% ($p < 0.01$), respectively. In contrast, the administration of CXE or XAN resulted in a significant recovery of the expression of PPARγ, C/EBP α, and SREBP-1c (Fig. 3B).

3.4. CXE and XAN modulated adipokine production in CT26-bearing mice

In the epididymal adipose tissue of the CC group, a significant decrease in leptin mRNA levels ($p < 0.01$) and a substantial increase in adiponectin expression (14.9-fold, $p < 0.01$) were observed compared to expression patterns of the control group (Fig. 4). The administration of CXE resulted in a significant and dose-dependent increase in suppressed leptin levels. Specifically, the CC + CXE50, CC + CXE100, and CC + XAN15 groups showed 5.6-fold, 5.8-fold, and 5.1-fold enhancement in leptin mRNA levels, respectively, compared to the CC group. In contrast, both CXE and XAN administration resulted in significant downregulation ($p < 0.01$) of adiponectin mRNA expression in the CT26-bearing mice (Fig. 4).

3.5. CXE and XAN modulated AMPK expression in CT26-bearing mice

As shown in Fig. 5, the phosphorylation level of AMPK in WAT of the CC group was significantly elevated, indicating a key mechanism in the pathogenesis of cachexia. The observed upregulation was considerably diminished following a consistent 7-day oral administration of CXE or XAN (Fig. 5).

4. Discussion

The main feature of cancer cachexia is extensive loss of skeletal muscle and adipose tissue, leading to progressive weight loss.[1] In this study, the CT26 colon cancer model was established to evaluate the attenuative effects of CXE and XAN on cancer-associated adipose atrophy. The cachectic phenotypes adipose tissue mass, tumor weight, and body weight were measured to evaluate the progression of cachexia. These phenotypes deteriorated in the CT26-bearing mice compared to the healthy ones, indicating that the cancer cachexia model was successfully established. In addition, CXE and XAN significantly improved body weight while ameliorating tumor-free body weight loss and epididymal adipose loss without affecting tumor burden (Fig. 1A, 1C, 1D). As shown in Fig. 1D, the 100 mg/kg CXE administered group effectively restored epididymal fat weight, whereas the effect of fat recovery in the XAN15 group was not statistically significant. In this study, the 7-day administration with CXE and XAN post-tumor inoculation might not have been insufficient for observing significant adipose tissue restoration, suggesting the potential benefits of extended treatment periods to reveal the efficacy of XAN in adipose recovery. This study demonstrated the influence of CXE and XAN on molecular pathways, such as lipolysis, WAT browning, lipogenesis, adipokine production, and adipocyte differentiation, underscoring the importance of further investigations into how varying durations of administration or concentrations might impact these processes. Therefore, future studies should be conducted to evaluate the effects of extended treatment durations of XAN to determine its optimal administration period for adipose tissue recovery. The present study provided insights into the preventive effects of CXE and XAN by evaluating key cachectic symptoms such as body weight, tumor-free weight, and epididymal adipose tissue weight. However, one limitation was the absence of detailed histological data on adipose tissue, which would have provided a more comprehensive understanding of the effects of CXE and XAN at the cellular level. Therefore, future studies should investigate histological analyses of adipose tissue, specifically focusing on the size of the fat droplets and markers of fat browning in adipose tissue, such as mitochondria in adipocytes. This approach aims

to explore deeper into the cellular mechanisms influenced by CXE and XAN, providing a more comprehensive understanding of their effects on adipose tissue.

Although previous studies have revealed the antitumor activities of CXE and XAN,[11] no statistical difference in tumor mass was observed among CXE- and XAN-treated groups in this study (Fig. 1B). Since pharmacokinetics and pharmacodynamics are critically affected by the administration route,[13] the method of supplementation might underly this inconsistency. Choi et al.[14] reported that the intraperitoneal (IP) administration of xanthorrhizol produced antitumor and anti-metastasis effects in B16BL6/CT26 tumor-bearing mice. In the present study, CT26-bearing mice were orally administered CXE and XAN, and administration had no inhibitory effect on cancer progression. IP administration was associated with almost 6-fold higher drug bioavailability and 4-fold shorter time to achieving peak plasma concentration compared to oral administration.[13] These promising results suggest that CXE and XAN attenuated cancer cachexia-induced adipose tissue loss without affecting tumor growth.

Although previous research has predominantly focused on skeletal muscle loss, recent studies have begun to emphasize the significance of adipose tissue wasting in the progression of cancer cachexia. Cancer-induced adipose depletion is primarily driven by altered lipid metabolism and adipose tissue browning.[4] Both clinical and preclinical studies have reported the activation of lipolysis as a key characteristic of cancer cachexia, driven by the sequential actions of the rate-limiting lipases ATGL and HSL. The upregulated lipolytic pathway, indicated by elevated protein expression of phosphorylated HSL and ATGL, has been observed in the WAT of cachectic cancer patients and tumor-bearing mice, leading to the depletion of fat mass.[15–17] Further, inhibiting lipolytic pathways via genetic ablation of HSL and ATGL genes has been proven to preserve adipose tissue mass in tumor-bearing mice.[18] Consistent with previous studies, this study also demonstrated an increase in phosphorylated HSL and ATGL levels in tumor-bearing mice, while CXE and XAN administration significantly suppressed lipolysis-related enzyme expression (Fig. 2A).

In addition to lipolysis, the progression of cancer cachexia is also associated with WAT browning, characterized by the overexpression of the thermogenic genes UCP1 and PGC-1a. This browning process significantly augments energy expenditure and thermogenesis within adipose tissue.[19] In a preclinical study conducted on LLC- and CT26-bearing mice, upregulated expression of UCP1 and PGC-1α induced browning in WAT.[20] Further, a subsequent clinical trial demonstrated that cachectic cancer patients showed increased UCP1 staining, indicative of enhanced thermogenesis in WAT.[20] In this study, a substantial increase in UCP1 and PGC-1a mRNA expression was triggered by the CT26 tumor, promoting thermogenesis within adipose tissue. However, upon administration of CXE or XAN, the expression of browning-related genes markedly declined, suggesting that both CXE and XAN have the potential to suppress the pathological browning of adipose tissue (Fig. 2B). Overall, these results revealed that supplementation with CXE or XAN considerably suppressed lipolysis and WAT browning in cachectic mice.

Besides lipolysis and WAT browning, adipose atrophy in cancer cachexia also involves impaired de novo lipogenesis and adipogenesis, leading to a reduction in lipid deposition and synthesis within adipocytes.[21] This impairment, characterized by decreased expression of lipogenic and adipogenic transcription factors, has been associated with diminished adipocyte size and fat mass in various cancer cachexia models.[4] A previous study showed significant downregulation of the key lipogenic enzyme LPL and adipogenic factors like PPARγ, C/EBPα, and SREBP-1c in the subcutaneous tissue of S180-bearing mice.[22] In colorectal cancer patients, peritumoral adipose tissue exhibited significantly reduced mRNA expression and activity of LPL and FAS,[23] indicating that stimulating de novo lipogenesis and adipogenic function could be a potential therapeutic strategy for mitigating adipose wasting in cancer cachexia. Consistent with other studies, this study observed a signifi-

cant decrease in the expression of lipogenic enzymes and adipogenesis-related factors in CT26-bearing mice. However, administration of CXE or XAN led to the recovery of the expression of LPL, FAS, and ACC, as well as the adipogenic factors PPARγ, C/EBPα, and SREBP-1c in epididymal fat tissue (Fig. 3). These findings highlight the therapeutic potential of CXE and XAN in preserving adipose tissue, primarily through enhancing the functions of lipogenesis and adipogenesis.

Cancer cachexia prompts the impairment of adipokine synthesis and secretion, including that of leptin and adiponectin.[19] While the exact role of adipokines in cancer cachexia remains elusive, their significance in regulating metabolic processes, inflammation, and immune responses suggests that their dysregulation could contribute to the development of cachexia. Several studies have reported altered circulating levels of adipokines in cachectic cancer patients and animal models. Specifically, Smiechowska et al.[24] found elevated serum adiponectin and reduced leptin levels among cachectic cancer patients in comparison to healthy subjects, and a preclinical study revealed a pronounced reduction in leptin mRNA expression in the epididymal fat tissue of MAC16-bearing mice.[24, 25] Consistent with previous studies, this study observed a significant reduction in leptin mRNA levels and a notable increase in adiponectin expression in tumor-bearing mice compared to the control group (Fig. 4), indicating dysregulation of adipokine synthesis. However, the administration of CXE or XAN effectively attenuated these changes by modulating adipokine expression (Fig. 4). Overall, these results suggest that CXE and XAN have the potential to restore disrupted adipokine production in CT26-bearing mice.

AMPK is a central metabolic regulator, maintaining cellular energy homeostasis in adipose tissue through the modulation of lipid metabolism, mitochondrial biogenesis, and adipokine expression. Under cachectic conditions, the hyperactivation of AMPK disrupts the balance of energy production and consumption, accelerating the progression of adipose tissue wasting and subsequent weight loss.[26] Specifically, in cachectic mice, activation of the AMPK pathway triggers enhanced lipolysis and thermogenesis within WAT.[26, 27] Liu et al.[28] reported that inactivating AMPK with Coix seed oil suppressed lipolysis by decreasing levels of phosphorylated HSL. Similarly, Lu et al.[27] demonstrated that carnosol mitigated tumor-induced lipolysis and lipid mobilization by suppressing the AMPK signaling pathway. Since lipolysis and the browning of WAT are essential pathogenic factors in cancer cachexia, therapeutic strategies focused on AMPK inactivation could be crucial in preserving adipose tissue. In this study, the protein expression of phosphorylated AMPK was markedly elevated in the cachexia model, and both CXE- and XAN-treated mice showed significant inhibition of AMPK expression (Fig. 5). These results suggest that the therapeutic potential of CXE and XAN in mitigating lipolysis and WAT browning may be derived from their inhibitory effect on the AMPK pathway. The NF-κB signaling pathway emerges as a crucial regulator of lipolysis.[29] Notably, the presence of an NF-κB inhibitor has demonstrated a significant reduction in TNF-α-mediated lipolysis.[30] Given the pivotal role of the NF-κB pathway in regulating lipolysis, it is essential to conduct a comprehensive examination in future studies. Although this study predominantly focused on the AMPK pathway and key factors in lipolysis and lipid utilization pathways, the molecular mechanisms of NF-κB need to be elucidated by assessing the expression of its downstream elements, like p65. Therefore, future research should investigate the NF-κB pathway to determine its potential influence on cancer-associated lipolysis, especially in the context of the effects of CXE and XAN.

Overall, these findings suggest that CXE and XAN could have therapeutic potential for use in treatments against cancer-associated adipose atrophy.

Author contributions

Haeun Kim: Conceptualization, Methodology, Investigation, Formal analysis, Writing – original draft. **Dong-Woo Lee:** Methodology, Investi-

gation, Formal analysis, Writing – review & editing. **Jae-Kwan Hwang:** Conceptualization, Formal analysis, Writing – review & editing.

Conflict of interest

The authors declare that there are no conflicts of interest.

Funding

None.

Ethical statement

The experimental protocol was approved by the Institute of Animal Care and Use Committee (IACUC) of Yonsei University (Seoul, Korea) (IACUC-202212-1592-02) to ensure ethical treatment of the animals.

Data availability

The data associated with this study can be made available upon reasonable request to the corresponding author.

Supplementary materials

Supplementary material associated with this article can be found, in the online version, at doi:10.1016/j.imr.2023.101020.

References

1. Ni J, Zhang L. Cancer cachexia: definition, staging, and emerging treatments. *Cancer Manag Res*. 2020;12:5597–5605.
2. Rohm M, Schäfer M, Laurent V, Üstünel BE, Niopek K, Algire C, et al. An AMP-activated protein kinase–stabilizing peptide ameliorates adipose tissue wasting in cancer cachexia in mice. *Nat Med*. 2016;22(10):1120–1130.
3. Antoun S, Bayar A, Ileana E, Laplanche A, Fizazi K, di Palma M, et al. High subcutaneous adipose tissue predicts the prognosis in metastatic castration-resistant prostate cancer patients in post chemotherapy setting. *Eur J Cancer*. 2015;51(17):2570–2577.
4. Dalal S. Lipid metabolism in cancer cachexia. *Ann Palliat Med*. 2018;8(1):13–23.
5. Rahmat E, Lee J, Kang Y. Javanese turmeric (*Curcuma xanthorrhiza* Roxb.): ethnobotany, phytochemistry, biotechnology, and pharmacological activities. *Evid Based Complement Alternat Med*. 2021;2021:9960813.
6. Kim MB, Kim C, Song Y, Hwang JK. Antihyperglycemic and anti-inflammatory effects of standardized *Curcuma xanthorrhiza* Roxb. extract and its active compound xanthorrhizol in high-fat diet-induced obese mice. *Evid Based Complement Alternat Med*. 2014;2014:205915.
7. Kook KE, Kim C, Kang W, Hwang JK. Inhibitory effect of standardized *Curcuma xanthorrhiza* supercritical extract on LPS-induced periodontitis in rats. *J Microbiol Biotechnol*. 2018;28(10):1614–1625.
8. Oon SF, Nallappan M, Tee TT, Shohaimi S, Kassim NK, Sa'ariwijaya MS, et al. Xanthorrhizol: a review of its pharmacological activities and anticancer properties. *Cancer Cell Int*. 2015;15:100.
9. Park JH, Jung YJ, Shrestha S, Lee SM, Lee TH, Lee CH, et al. Inhibition of NO production in LPS-stimulated RAW264.7 macrophage cells with curcuminoids and xanthorrhizol from the rhizome of *Curcuma xanthorrhiza* Roxb. and quantitative analysis using HPLC. *J Korean Soc Appl Biol Chem*. 2014;57:407–412.
10. Park JH, Park KK, Kim MJ, Hwang JK, Park SK, Chung WY. Cancer chemoprotective effects of *Curcuma xanthorrhiza*. *Phytother Res*. 2008;22(5):695–698.
11. Simamora A, Timotius KH, Yerer MB, Setiawan H, Xanthorrhizol Mun'im A. a potential anticancer agent, from *Curcuma xanthorrhiza* Roxb. *Phytomedicine*. 2022;105:154359.
12. Kim SH, Hong KO, Hwang JK, Park KK. Xanthorrhizol has a potential to attenuate the high dose cisplatin-induced nephrotoxicity in mice. *Food Chem Toxicol*. 2005;43(1):117–122.
13. Al Shoyaib A, Archie SR, Karamyan VT. Intraperitoneal route of drug administration: should it be used in experimental animal studies? *Pharm Res*. 2019;37(1):12.
14. Choi MA, Kim SH, Chung WY, Hwang JK, Park KK. Xanthorrhizol, a natural sesquiterpenoid from *Curcuma xanthorrhiza*, has an anti-metastatic potential in experimental mouse lung metastasis model. *Biochem Biophys Res Commun*. 2005;326(1):210–217.
15. Agustsson T, Rydén M, Hoffstedt J, van Harmelen V, Dicker A, Laurencikiene J, et al. Mechanism of increased lipolysis in cancer cachexia. *Cancer Res*. 2007;67(11):5531–5537.
16. Xie H, Heier C, Meng X, Bakiri L, Pototschnig I, Tang Z, et al. An immune-sympathetic neuron communication axis guides adipose tissue browning in cancer-associated cachexia. *Proc Natl Acad Sci USA*. 2022;119(9):e2112840119.
17. Silvério R, Lira FS, Oyama LM, Oller do Nascimento CM, Otoch JP, Alcântara PSM, et al. Lipases and lipid droplet-associated protein expression in subcutaneous white adipose tissue of cachectic patients with cancer. *Lipids Health Dis*. 2017;16(1):1–11.
18. Das SK, Eder S, Schauer S, Diwoky C, Temmel H, Guertl B, et al. Adipose triglyceride lipase contributes to cancer-associated cachexia. *Science*. 2011;333(6039):233–238.
19. Mannelli M, Gamberi T, Magherini F, Fiaschi T. The adipokines in cancer cachexia. *Int J Mol Sci*. 2020;21(14):4860.
20. Petruzzelli M, Schweiger M, Schreiber R, Campos-Olivas R, Tsoli M, Allen J, et al. A switch from white to brown fat increases energy expenditure in cancer-associated cachexia. *Cell Metab*. 2014;20(3):433–447.
21. Joshi M, Patel BM. The burning furnace: alteration in lipid metabolism in cancer-associated cachexia. *Mol Cell Biochem*. 2022;477:1709–1723.
22. Du L, Yang YH, Wang YM, Xue CH, Kurihara H, Takahashi K. EPA-enriched phospholipids ameliorate cancer-associated cachexia mainly via inhibiting lipolysis. *Food Funct*. 2015;6(12):3652–3662.
23. Notarnicola M, Miccolis A, Tutino V, Lorusso D, Caruso MG. Low levels of lipogenic enzymes in peritumoral adipose tissue of colorectal cancer patients. *Lipids*. 2012;47(1):59–63.
24. Smiechowska J, Utech A, Taffet G, Hayes T, Marcelli M, Garcia JM. Adipokines in patients with cancer anorexia and cachexia. *J Investig Med*. 2010;58(3):554–559.
25. Bing C, Bao Y, Jenkins J, Sanders P, Manieri M, Cinti S, et al. Zinc-alpha2-glycoprotein, a lipid mobilizing factor, is expressed in adipocytes and is up-regulated in mice with cancer cachexia. *Proc Natl Acad Sci USA*. 2004;101(8):2500–2505.
26. Shen Q, Miao CX, Zhang WL, Li YW, Chen QQ, Li XX, et al. SiBaoChongCao exhibited anti-fatigue activities and ameliorated cancer cachexia in mice. *RSC Adv*. 2019;9(30):17440–17456.
27. Lu S, Li Y, Shen Q, Zhang W, Gu X, Ma M, et al. Carnosol and its analogues attenuate muscle atrophy and fat lipolysis induced by cancer cachexia. *J Cachexia Sarcopenia Muscle*. 2021;12(3):779–795.
28. Liu H, Li L, Zou J, Zhou T, Wang B, Sun H, et al. Coix seed oil ameliorates cancer cachexia by counteracting muscle loss and fat lipolysis. *BMC Complement Altern Med*. 2019;19(1):267.
29. Baazim H, Antonio-Herrera L, Bergthaler A. The interplay of immunology and cachexia in infection and cancer. *Nat Rev Immunol*. 2022;22(5):309–321.
30. Miao C, Lv Y, Zhang W, Chai X, Feng L, Fang Y, et al. Pyrrolidine dithiocarbamate (PDTC) attenuates cancer cachexia by affecting muscle atrophy and fat lipolysis. *Front Pharmacol*. 2017;8:915.